

## Control factor of solar cycle variation of auroral kilometric radiation

Atsushi Kumamoto<sup>1</sup>, Takayuki Ono<sup>1</sup>, Masahide Iizima<sup>1</sup> and Hiroshi Oya<sup>2</sup>

<sup>1</sup> *Department of Geophysics, Graduate School of Science, Tohoku University,  
Aoba, Aramaki, Aoba-ku, Sendai 980-8578*

<sup>2</sup> *Department of Space Communications, Faculty of Engineering,  
Fukui University of Technology, 3-6-1, Gakuen, Fukui 910-8505*

(Received December 25, 2002; Accepted June 5, 2003)

**Abstract:** Solar cycle variations of auroral kilometric radiation (AKR) observed by the Akebono satellite have been compared with the variations of F10.7 and solar wind dynamic pressure. F10.7 and solar wind dynamic pressure show different solar cycle variations: F10.7 increases during solar maximum and decreases during solar minimum. Solar wind dynamic pressure suddenly increases in the declining phase of solar activity and gradually decreases. The pressure minimum occurs during solar maximum. Statistical analysis of the Akebono data has shown that AKR occurrence minimum occurs during solar maximum, however AKR occurrence maximum coincides not with solar wind dynamic pressure peak but with F10.7 minimum. Up-flowing ion (UFI) events and ambient plasma density, which are associated with generation conditions of AKR, also show similar behavior. They are dependent not on solar wind dynamic pressure but on F10.7. These results suggest the anti-correlation between discrete aurora and solar activities, which has been never recognized through the studies on secular variations of auroral phenomena mainly based on old auroral records obtained in mid-latitude regions.

**key words:** auroral kilometric radiation, seasonal variation, solar cycle variation, up-flowing ion event, the Akebono (EXOS-D) satellite

### 1. Introduction

The correlation between auroral activity and solar activity has been recognized since the 18th century. In 1716, aurora came back again to Europe after long absence and surprised people in the era. The year coincides with the end of grand minimum of sunspot number and solar activity, which is called Maunder Minimum. It is now known that there were some grand minimum periods of solar activity, such as Wolf Minimum (1290–1350), Sporer Minimum (1450–1540), Maunder Minimum (1645–1715), Dalton Minimum (1790–1825), and Modern Minimum (1901–1913) (Dalton, 1803, 1834; Wolf, 1856, 1868; Sporer, 1889; Maunder, 1894; Eddy, 1976a, b). It has been also reported that aurora occurrence decrease during those periods (De Mairan, 1733; Fritz, 1873; Eddy, 1976a, b; Siscoe, 1980). The 11-year variation of sunspot number was discovered in the middle of the 19th century (Schwabe, 1843). Soon after that, it was also pointed out that aurora occurrence shows the similar 11-year variation

(Loomis, 1873; Tromholt, 1902). Therefore, it is now widely accepted that auroral phenomena becomes active when the solar activity increases.

However, recent statistical studies have reported seasonal variations of auroral phenomena; electron precipitation (Newell *et al.*, 1996, 1999; Morooka and Mukai, 2003), auroral kilometric radiation (Kasaba *et al.*, 1997; Kumamoto and Oya, 1998), upflowing ions (Collin *et al.*, 1998; Morooka and Mukai, 2003), auroral UV emissions (Liou *et al.*, 1997, 2001), electromagnetic electron cyclotron (EMIC) waves (Elandson and Zanetti, 1998), cosmic radio noise absorption (CNA) events (Yamagishi *et al.*, 1998), and AE index (Lyatsky *et al.*, 2001; Benkevitch *et al.*, 2002). They all are quiet in the summer polar region and active in the winter polar region. Therefore it is suggested that auroral phenomena are affected not only by solar activity but also by the ionospheric conditions. In addition, based on the long-term observation by the Akebono satellite, it has been clarified that occurrence frequency of auroral kilometric radiation (AKR) becomes small not during solar minimum but during solar maximum (Kumamoto, 2000; Kumamoto *et al.*, 2003). AKR is known as the phenomena, which are closely related to discrete auroral arcs (Gurnett, 1974; Kurth and Gurnett, 1975; Benson and Akasofu, 1984; Huff *et al.*, 1988) and the auroral electron acceleration processes (Green *et al.*, 1979). Close correlations between AKR activity and geomagnetic indices such as *AE*, *Kp* and *Dst* have been also pointed out by previous studies (Gurnett, 1974; Voots *et al.*, 1977; Murata *et al.*, 1997; Kurth and Gurnett, 1998). The results by the Akebono satellite seem to contradict the common knowledge that activities of aurora and AKR show in-phase relation with solar activity. Therefore, explanations for the results have come to be needed. As for the control mechanisms, we have suggested that increase of ambient plasma density during solar maximum hinders the development of field aligned potential differences (Kumamoto *et al.*, 2003), which is also suggested as control mechanism of AKR seasonal variation (Kumamoto and Oya, 1998; Kumamoto, 2000; Kumamoto *et al.*, 2001, 2003). However, it is also pointed out as another candidate that AKR is controlled by solar wind dynamic pressure which becomes minimum not during solar minimum but in solar maximum. Based on the long-term observations by IMP 8 and Voyager 2, solar wind dynamic pressure minimum is near solar maximum and the peak pressure occurs 1–2 years later (Richardson *et al.*, 1995; Richardson and Wang, 1999).

In this paper, we have investigated solar cycle variation of AKR observed by the Akebono satellite and compared them with solar cycle variations of F10.7 and solar wind dynamic pressure. Furthermore, the solar cycle dependences of up-flowing ion (UFI) events and ambient plasma density, which are associated with generation conditions of AKR, have been also analyzed. Then, control factors of solar cycle variations of them have been discussed based on the results. In Section 2, we describe the data sets and the analysis method of AKR, UFI, and ambient plasma density. The results are presented in Section 3, and the discussion and conclusions are given in Section 4.

## 2. Data sets and methods of analysis

The occurrence probability of AKR in the summer and winter polar regions were calculated based on the Akebono plasma wave and sounder (PWS) data obtained from

1989 to 2002. The PWS instrumentation has been described by Oya *et al.* (1990). The wave data observed in geomagnetic latitudes higher than  $45^\circ$  in a sector from 1500 to 0300 MLT were utilized. Frequency range from 100 kHz to 1 MHz was divided into 32 frequency range bins, and an occurrence probability of AKR was calculated for each frequency bin. An occurrence of AKR was defined by an intensity larger than  $-150$  dBW/m<sup>2</sup>Hz. The intensity level is sufficiently large to exclude other wave components such as solar radio bursts. However, saturation components of AKR in lower frequency range are difficult to be excluded from the analysis. Therefore, it is supposed that occurrence probabilities are slightly overestimated especially in high frequency range. Assuming AKR is generated in the electron cyclotron frequency at the source and propagates upward, the wave data below the electron cyclotron frequency at the satellite were not utilized for the analysis. Since it has been clarified that AKR occurrence probability shows distinct seasonal dependence (Kumamoto and Oya, 1998; Kumamoto, 2000; Kumamoto *et al.*, 2001), the data observed in the summer and winter polar region were analyzed separately. In this paper, the summer and winter seasons are defined as the 120 day intervals around the solstice.

The occurrence probabilities of UFI events in the summer and winter polar regions were calculated based on Akebono low energy particle (LEP) data obtained from 1989 to 1997. The LEP instrumentation has been described by Mukai *et al.* (1990). Based on the early observations (Shelley *et al.*, 1976; Ghielmetti *et al.*, 1978; Gorney *et al.*, 1981), UFI events have been known as the phenomena that  $H^+$ ,  $O^+$  and other ions in energy range up to a few keV are upflowing from auroral and polar cap ionosphere. They are divided into two categories: ion beam components with small pitch angle and ion conic components with large pitch angle. Depending on whether to focus on, various identification criteria were used for the statistical studies of UFI (Yau *et al.*, 1984, 1985; Collin *et al.*, 1988, 1998; Morooka and Mukai, 2003). In this paper, focusing on auroral ion beam components produced by the field-aligned potential drops, UFI events were identified using the following method. First, the energetic ion data were divided into 15 bins for three pitch angle ranges and five energy ranges, as shown in Table 1. Then, the average number flux of each bin was calculated to identify UFI events using the following criteria; (1) average number flux of greater than 1.22 keV ions in the upgoing sector ( $U_4$ ,  $U_5$ ) is greater than  $1.4 \times 10^6$  eV/(cm<sup>2</sup>s·sr·eV), (2) in the upgoing sector, average number flux of greater than 1.22 keV ions ( $U_4$ ,  $U_5$ ) is 1.3 times greater than that of lower energy ions ( $U_1$ ,  $U_2$ ,  $U_3$ ), and (3) average number flux of

Table 1. Fifteen data bins, divided into three pitch angle ranges and five energy ranges, used to calculate average number fluxes of energetic ions.

	0–30° (Up)	30–60° (Perp.)	60–90° (Down)
34.6–124 eV	$U_1$	$P_1$	$D_1$
124–343 eV	$U_2$	$P_2$	$D_2$
343 eV–1.22 keV	$U_3$	$P_3$	$D_3$
1.22–3.39 keV	$U_4$	$P_4$	$D_4$
3.39–12.1 keV	$U_5$	$P_5$	$D_5$

upgoing ions in energy range greater than 1.22 keV ( $U_4$ ,  $U_5$ ) is 1.3 times greater than that of ions with downgoing ( $D_4$ ,  $D_5$ ) or perpendicular ( $P_4$ ,  $P_5$ ) pitch angle. Energetic ion data observed in invariant latitude ranges from 65 to 75° in a sector from 1800 to 2400 MLT below an altitude of 7000 km were utilized.

Ambient plasma densities in the summer and winter polar regions were derived from the Akebono PWS data obtained in invariant latitude ranges from 65 to 75° in a sector from 1800 to 2400 MLT. Upper limit frequencies of upper hybrid resonance (UHR) waves and whistler waves were utilized for determination of plasma frequencies at the observation points. Then, number density of ambient plasma was derived from plasma frequency at each observation point.

### 3. Results

In Fig. 1, solar cycle variations of 1-month averaged sunspot number and F10.7, 3-month averaged solar wind dynamic pressure, and occurrence probability of AKR in the summer and winter polar regions are displayed. Solar wind dynamic pressure was calculated from ion number density and plasma flow speed. In Fig. 1d and 1e, total occurrence probabilities of summer and winter AKR in a frequency range from 100 to 500 kHz for each year are displayed by histograms. Gray indicates the year in which total observation time is shorter than 100 hour. In Fig. 1f and 1g, the left and right vertical axis respectively indicate AKR emission frequency and AKR source altitude determined by assuming that AKR is generated in electron cyclotron frequency in the source regions located in an invariant latitude of 70°. The occurrence probabilities of AKR are shown by color scale. Black indicates no data coverage. Sunspot number and F10.7 clearly show the similar 11-years variations: They increase during solar maximum (around 1989 and 2000) and decrease during solar minimum (around 1994–1995). As shown by Richardson *et al.* (1995), solar wind dynamic pressure shows different 11-year variation: The pressure peak occurs in declining phase of solar activity and gradually decreases. It becomes minimum around solar maximum. The solar cycle variations of AKR occurrence shown in Fig. 1 are basically similar with results of Kumamoto *et al.* (2003). It may appear that AKR occurrence becomes minimum when solar wind dynamic pressure is minimum. However the AKR occurrence maximum does not coincide with the pressure maximum in declining phase of solar activity. It seems more reasonable to interpret the variation as an anti-correlation with sunspot number and F10.7.

The vertical profiles of UFI occurrence probability in the three periods, 1989–1992 (solar maximum), 1991–1994 (declining phase of solar activity), and 1994–1997 (solar minimum), are shown in Fig. 2. In the both summer and winter polar regions, occurrence probabilities of UFI events during solar maximum are smaller than those during solar minimum in all altitude range, as shown by Kumamoto *et al.* (2003). However, extreme vertical profiles are not seen during the declining phase of solar activity, when the solar wind dynamic pressure peak appears. It suggests that vertical distribution of auroral particle acceleration region depends not on solar wind dynamic pressure but on the solar flux indicated by F10.7.

Figure 3 shows vertical profiles of ambient plasma density during 1989–1992 (solar

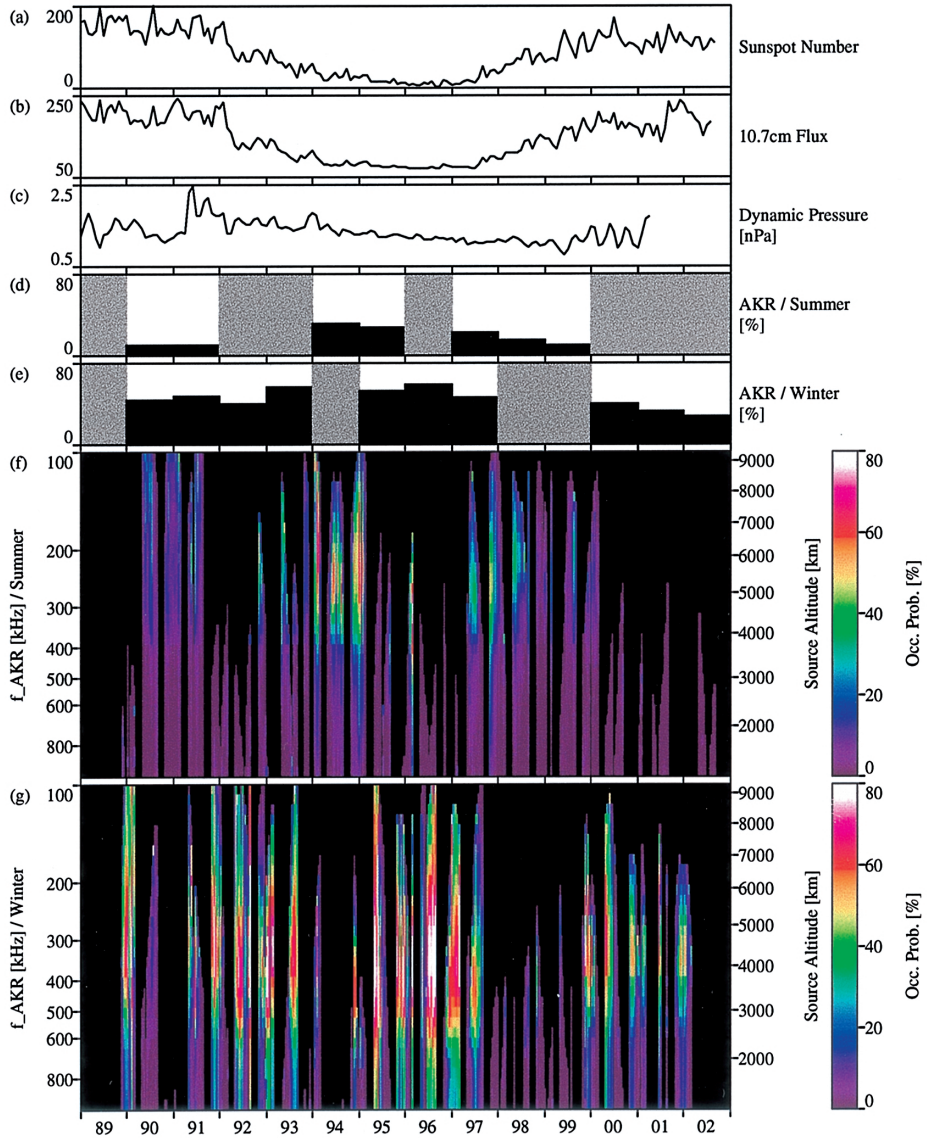


Fig. 1. Solar cycle variations of (a) 1-month averaged sunspot number, (b) 1-month averaged F10.7, (c) 3-month averaged solar wind dynamic pressure, and (d-g) occurrence probability of AKR in the summer and winter polar regions. In Fig. 1d and 1e, total occurrence probabilities of summer and winter AKR in a frequency range from 100 to 500 kHz for each year are displayed by histograms. Gray indicates the year in which total observation time is shorter than 100 hour. In Fig. 1f and 1g, the left and right vertical axis respectively indicate the emission frequency of AKR and AKR source altitude determined by assuming that AKR are generated in electron cyclotron frequency in the source regions located in an invariant latitude of  $70^\circ$ . The occurrence probabilities of AKR are shown by color scale. Black indicates no data.

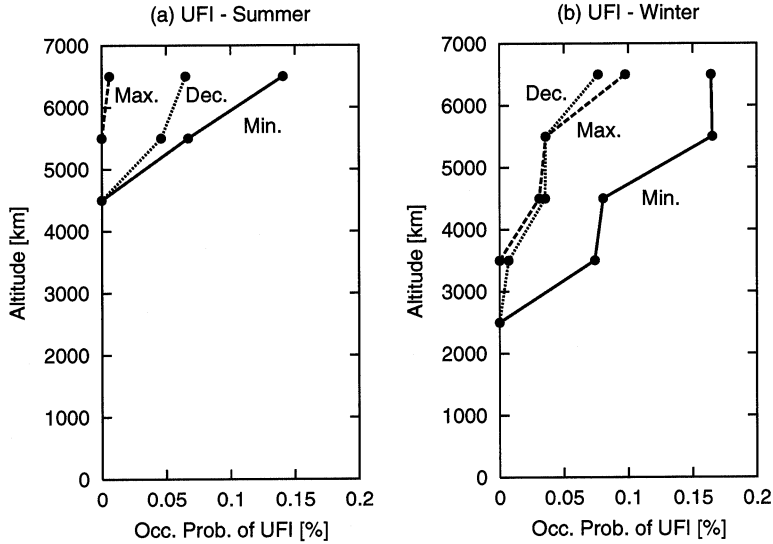


Fig. 2. The vertical profiles of UFI occurrence probability in the (a) summer and (b) winter polar regions. “Max.,” “Dec.,” and “Min.” indicate the periods of 1989–1992 (solar maximum), 1991–1994 (declining phase of solar activity), and 1994–1997 (solar minimum), respectively.

maximum), 1991–1994 (declining phase of solar activity), and 1994–1997 (solar minimum). Ambient plasma densities during solar minimum shows knee-like profile which consists of ionospheric cold plasma component and magnetospheric hot plasma component, as reported by previous studies (Mozer *et al.*, 1979; Hilgers, 1992; Persoon *et al.*, 1993; Kletzing and Torbert, 1994; Kletzing *et al.*, 1998). During solar maximum, on the other hand, ambient plasma densities are so scattered to large values that knee-like profile almost disappears. However, extreme profiles are not seen in the declining phase of solar activity, which is different from the behavior of solar wind dynamic pressure but similar to the behaviors of AKR, UFI and F10.7. It is also pointed out that the solar cycle variation of ambient plasma density occurs not only in the ionosphere but also up to an altitude about 8000 km, where AKR sources and auroral particle acceleration regions are mainly generated.

#### 4. Discussion and conclusions

The results shown in this paper distinctly suggest that the solar cycle variations of AKR and UFI are caused not by the variation of solar wind dynamic pressure but by the variation of solar flux indicated by sunspot number and F10.7. During solar maximum, when solar flux increases, occurrence probabilities of AKR and UFI decrease in the both summer and winter polar regions. Ambient plasma density also shows clear solar cycle dependence. During solar maximum, ambient plasma density not only in the ionosphere but also up to an altitude about 8000 km, where AKR sources and auroral particle acceleration regions are generated, becomes large probably due to

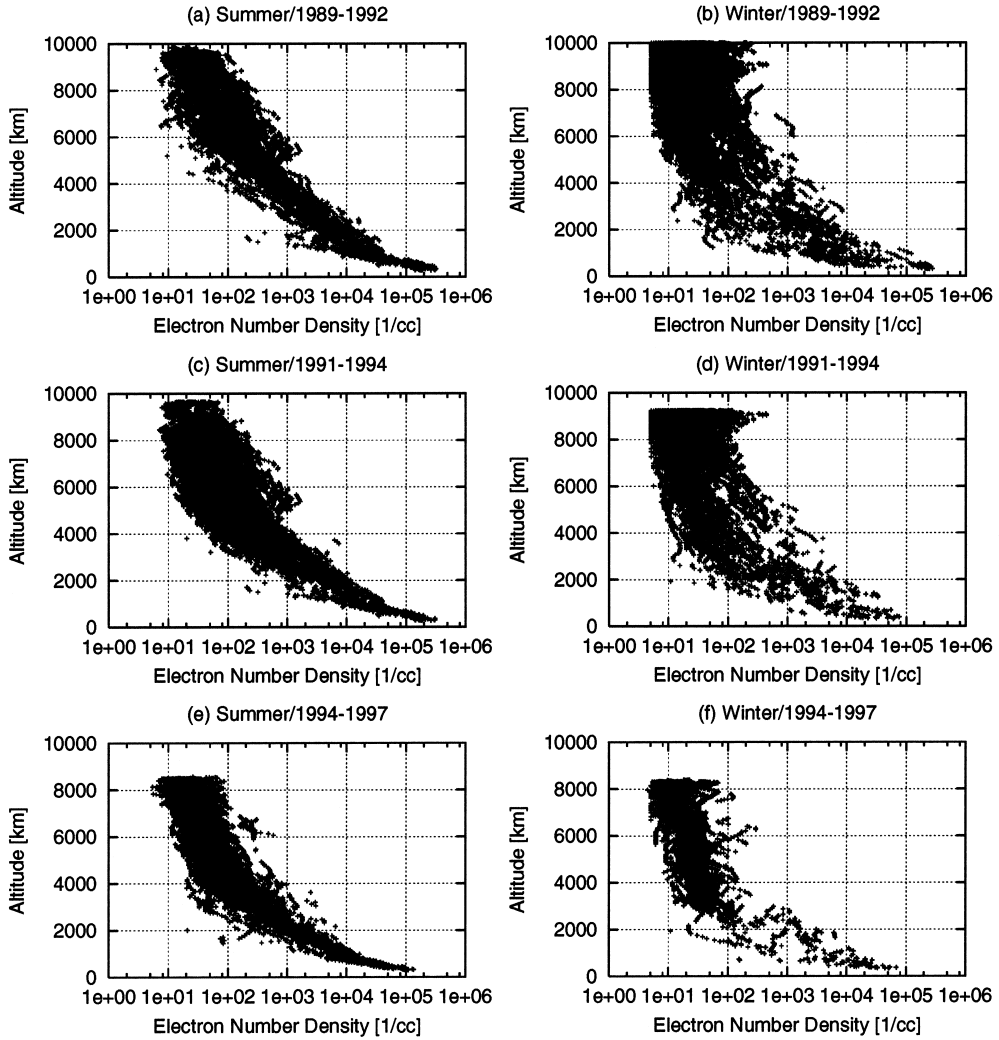


Fig. 3. Vertical profiles of ambient plasma density during (a, b) 1989–1992 (solar maximum), (c, d) 1991–1994 (declining phase of solar activity), and (e, f) 1994–1997 (solar minimum). The left and right plots indicate the profiles in the (a, c, e) summer and (b, d, f) winter polar regions, respectively.

increase of upwelling plasma from the ionosphere. Therefore, it is strongly suggested that dense ambient plasma hinders the generation process of AKR sources and field-aligned potential differences during solar maximum. Based on cyclotron maser instability (CMI) theory, it is difficult to grow intense R-X mode AKR in dense ambient plasma (Wu and Lee, 1979; Hewitt *et al.*, 1982). In addition, assuming that field-aligned currents  $J$  is constant, it is expected that field-aligned drift velocity  $v_d = J/Ne$  decreases when ambient plasma density  $N$  increases. Then, plasma waves, such as ion-acoustic waves and electrostatic ion cyclotron (EIC) waves, can not be unstable

(Kindel and Kennel, 1971), and can not generate large field aligned potential differences. It has been suggested that the presence of a field aligned potential drop is important for generation of intense R-X mode AKR via CMI process (Fung and Vinas, 1994; Ergun *et al.*, 2000).

As for the other auroral phenomena, there have been reported some statistical analysis results which suggest anti-correlation with solar activity. Silverman (1992) has performed statistical analysis of auroral records in Greenland from 1841 to 1960 and pointed out that long-term variations of aurora occurrence in high-latitude regions are complicated and do not show simple in-phase relation with solar activity. In Fig. 21 of Silverman (1992), there are seen some aurora occurrence minima around 1884, 1894, and 1902, which correspond to solar maximum. Statistical studies of all sky camera data obtained in Northern Finland during 1974–1996 also show the results which suggest the anti-correlation between aurora occurrence and solar activity (Nevanlinna and Pulkkinen, 1998). In Fig. 2a of Nevanlinna and Pulkkinen (1998), occurrence of “quiet arcs” seems to decrease during solar maximum and increase during solar minimum. The authors did not point out the result because they mainly focused on in-phase relation between active aurora occurrence and solar activity. However, it suggests that AKR sources, UFI events, and auroral particle acceleration regions are mainly linked to stable discrete auroral arcs rather than to unstable active aurora. There are also some evidences which support the anti-correlation between auroral particle acceleration processes and solar activity. Newell *et al.* (1998) have reported that the occurrence area size of electron precipitations decreases during solar maximum based on 12 years of energetic electron data obtained by the DMSP satellite. Yau *et al.* (1985) have carried out the statistical analysis of UFI based on 4 years of energetic ion data obtained by the DE-1 satellite, and concluded that there is not seen clear solar cycle dependence of  $H^+$  and  $O^+$  except for  $O^+$  conics components, which increase during solar maximum. However, as seen in Fig. 6 of Yau *et al.* (1985),  $H^+$  and  $O^+$  with pitch angles of  $160\text{--}180^\circ$  during solar minimum seem slightly larger than those during solar maximum. Cattell *et al.* (1991) have carried out statistical analysis of electrostatic shocks observed by the S3-3 satellite, and pointed out that occurrence probability of electrostatic shocks with ion beams decrease in solar maximum. They also shows the solar cycle dependence of vertical profiles of electrostatic shocks with ion beams (Fig. 5a of Cattell *et al.*, 1991), which are consistent with UFI vertical profiles in our results. The solar cycle dependence of AL index clarified by Nakai and Kamide (1999) suggests the solar cycle dependence of auroral electrojets. During solar maximum, AL index becomes difficult to increase even when the solar wind parameter  $V^2B_z$  becomes large.

It seems inconsistent with the common knowledge that aurora phenomena become active during solar maximum. However, it is not discrepancy. The positive correlation between aurora occurrence and solar activity, known since the 18th century, has been established through the studies of aurora secular variations based on the auroral occurrence records in Europe, Northern America, East Asia, and Russia since ancient times (Lovering, 1867, 1868; Fritz, 1873; Matsushita, 1956; Link, 1962, 1964; Keimatsu, 1976; Stothers, 1979; Dall’Olmo, 1979; Loysha, 1989). Most of them were, however, made by naked-eye observations in the mid-latitude regions ( $< 60^\circ$  in geomagnetic



latitude). They probably include the both diffuse aurora generated by soft electrons with an energy range below a few 100 eV and discrete aurora generated by accelerated electrons with an energy range larger than a few keV, and mainly reflect the characteristics of the diffuse aurora in mid-latitude regions. On the other hand, AKR is mainly associated with discrete auroral arcs which are produced by accelerated auroral electrons. It does not seem strange that their solar cycle dependences are different. It should be noted that there is no contradiction between the results in this paper and previous studies which reported close correlation of AKR with geomagnetic indices such as *AE*, *Kp* and *Dst*. Based on the results by Lyatsky *et al.* (2001) and Benkevitch *et al.* (2002), which shows seasonal dependence of *AE* index, *AE* index is controlled by the ionospheric conditions. Therefore, it is assumed that *AE* index, or activity of auroral electrojets, shows anti-correlation with solar activity just as AKR, UFI and stable discrete auroral arcs. Relation between AKR activity and *Kp/Dst* indices is probably indirect. The results by Murata *et al.* (1997) were based on GEOTAIL wave data obtained in 1993. The question on long-term correlation between AKR activity and *Kp/Dst* indices is deferred to future investigations. More than 40 years has passed since the scientific measurements in the polar region and from the space were started. The paradigm of positive correlation between auroral occurrence and solar activity should be reinvestigated through the statistical studies based on the long-term observation data sets obtained by the methods in the new era.

### Acknowledgments

We would like to thank the staff of the Akebono satellite team. The Akebono LEP data were provided by T. Mukai through DARTS at Institute of Space and Astronautical Science (ISAS). The Sunspot number and F10.7 data were obtained from NOAA's National Geophysical Data Center. Solar-wind data were obtained from NASA's OMNI data facility.

The editor thanks the referees for their help in evaluating this paper.

### References

- Benkevitch, L.V., Lyatsky, W.B., Koustov, A.V., Sofko, G. J. and Hamza, A.M. (2002): Substorm onset times as derived from geomagnetic indices. *Geophys. Res. Lett.*, **29**, 10.1029/2001GL014386.
- Benson, R.F. and Akasofu, S.-I. (1984): Auroral kilometric radiation/aurora correlation. *Radio Sci.*, **19**, 527–541.
- Cattell, C.A., Chari, S. and Temerin, M.A. (1991): An S3-3 satellite study of the effects of the solar cycle on the auroral acceleration process. *J. Geophys. Res.*, **96**, 17903–17908.
- Collin, H., Peterson, W.K., Drake, J.F. and Yau, A.W. (1988): The helium components of energetic terrestrial ion upflows: their occurrence, morphology, and intensity. *J. Geophys. Res.*, **93**, 7558–7564.
- Collin, H., Peterson, W.K., Lennartsson, O.W. and Drake, J.F. (1998): The seasonal variations of auroral ion beams. *Geophys. Res. Lett.*, **25**, 4071–4074.
- Dall'Olmo, U. (1979): An additional list of auroras from European sources from 450 to 1466 AD. *J. Geophys. Res.*, **84**, 1525–1535.
- Dalton, J. (1803): *Meteorologische Beobachtungen*. *Ann. Phys.*, **15**, 197–198.
- Dalton, J. (1834): *Meteorological Observations and Essays*, 2nd ed. London, Baldwin and Gradock.
- De Mairan, J.J.D. (1733): *Traite Physique et Historique de l'Aurore Boreale*. Paris, Imprimerie Royale.

- Eddy, J.A. (1976a): The Maunder Minimum. *Science*, **192**, 1189–1202.
- Eddy, J.A. (1976b): The sun since Bronze Age. *Physics of Solar Planetary Environments*, ed. by D. J. Williams. Washington D.C., AGU, 958–972.
- Ergun, R.E., Carlson, C.W., McFadden, J.P., Delory, G.T., Strangeway, R.J. and Pritchett, P.L. (2000): Electron-cyclotron maser driven by charged-particle acceleration from magnetic field-aligned electric fields. *Astrophys. J.*, **538**, 456–466.
- Elandson, R.E. and Zanetti, L.J. (1998): A statistical study of auroral electromagnetic ion cyclotron waves. *J. Geophys. Res.*, **103**, 4627–4636.
- Fritz, H. (1873): *Verzeichniss Beobachter Polarlichter*. Wien, Austria.
- Fung, S.F. and Vinas, A.F. (1994): Excitation of high-frequency electromagnetic waves by energetic electrons with loss cone distribution in a field-aligned potential drop. *J. Geophys. Res.*, **99**, 8671–8686.
- Ghielmetti, A.G., Johnson, R.G., Sharp, R.D. and Shelley, E.G. (1978): The latitudinal, diurnal and altitudinal distributions of upward flowing energetic ions of ionospheric origin. *Geophys. Res. Lett.*, **5**, 59–62.
- Gorney, D.A., Clarke, J.A., Croley, D., Fennell, J.F., Luhmann, J. and Mizera, P. (1981): The distribution of ion beams and conics below 8000 km. *J. Geophys. Res.*, **86**, 83–89.
- Green, J.L., Gurnett, D.A. and Hoffman, R.A. (1979): A correlation between auroral kilometric radiation and inverted V electron precipitation. *J. Geophys. Res.*, **84**, 5216–5222.
- Gurnett, D.A. (1974): The earth as a radio source: Terrestrial kilometric radiation. *J. Geophys. Res.*, **79**, 4227–4238.
- Hewitt, R.G., Melrose, D.B. and Ronmark, K.G. (1982): The loss-cone driven electron-cyclotron maser. *Aust. J. Phys.*, **35**, 447–471.
- Hilgers, A. (1992): The auroral radiating plasma cavities. *Geophys. Res. Lett.*, **19**, 237–240.
- Huff, R.L., Calvert, W., Craven, J.D., Frank, L.A. and Gurnett, D.A. (1988): Mapping of auroral kilometric radiation sources to the aurora. *J. Geophys. Res.*, **93**, 11445–11454.
- Kasaba, Y., Matsumoto, H., Hashimoto, K. and Anderson, R.R. (1997): The angular distribution of auroral kilometric radiation observed by the GEOTAIL spacecraft. *Geophys. Res. Lett.*, **24**, 2483–2486.
- Keimatsu, M. (1976): A chronology of aurorae and sunspots observed in China, Korea and Japan, Part VII, A brief summary of the records from BC 687 to AD 1600. *Ann. Sci. Kanazawa Univ.*, **13**, 1–32.
- Kindel, J.M. and Kennel, C.F. (1971): Topside current instabilities. *J. Geophys. Res.*, **76**, 3055–3078.
- Kletzing, C.A. and Torbert, R.B. (1994): Electron time dispersion. *J. Geophys. Res.*, **99**, 2159–2172.
- Kletzing, C.A., Mozer, F.S. and Torbert, R.B. (1998): Electron temperature and density at high latitude. *J. Geophys. Res.*, **103**, 14837–14845.
- Kumamoto, A. (2000): A study on the source of auroral kilometric radiation based on the observations by the Akebono (EXOS-D) satellite. Ph. D. Thesis, Tohoku University.
- Kumamoto, A., Ono, T. and Oya, H. (2001): Seasonal dependence of the vertical distributions of auroral kilometric radiation sources and auroral particle acceleration regions observed by the Akebono satellite. *Adv. Polar Upper Atmos. Res.*, **15**, 32–42.
- Kumamoto, A. and Oya, H. (1998): Asymmetry of occurrence-frequency and intensity of AKR between summer polar region and winter polar region sources. *Geophys. Res. Lett.*, **25**, 2369–2372.
- Kumamoto, A., Ono, T., Iizima, M. and Oya, H. (2003): Seasonal and solar cycle variations of the vertical distribution of the occurrence probability of auroral kilometric radiation sources and of up-flowing ion events. *J. Geophys. Res.*, **108** (A1), 1032, doi: 10.1029/2002JA009522.
- Kurth, W.S. and Gurnett, D.A. (1998): Auroral kilometric radiation integrated power flux as proxy for AE. *Adv. Space Res.*, **22**, 73–77.
- Kurth, W.S., Baumbach, M.M. and Gurnett, D.A. (1975): Direction-finding measurements of auroral kilometric radiation. *J. Geophys. Res.*, **80**, 2764–2770.
- Link, F. (1962): *Observations et catalogue des aurores boreales apparues en occident de -626 a 1600*. *Geophys. Sb.*, **X**, 297–392.
- Link, F. (1964): *Observations et catalogue des aurores boreales apparues en occident de 1600 a 1700*. *Geophys. Sb.*, **XII**, 501–547.
- Liou, K., Newell, P.T., Meng, C.-I., Brittnacher, M. and Parks, G. (1997): Synoptic auroral distribution: A survey using Polar ultraviolet imagery. *J. Geophys. Res.*, **102**, 27197–27205.

- Liou, K., Newell, P.T. and Meng, C.-I. (2001): Seasonal effects on auroral particle acceleration and precipitation. *J. Geophys. Res.*, **106**, 5531–5542.
- Loomis, E. (1873): Comparison of the mean daily range of the magnetic declination and the number of auroras observed each year, with the extent of the black spots on the surface of the sun. *Am. J. Sci.*, Ser. 3, **5**, 245–260.
- Lovering, J. (1867): On the secular periodicity of the aurora borealis. *Mem. Am. Acad. Arts Sci.*, **9**, 101–111.
- Lovering, J. (1868): On the periodicity of the aurora borealis. *Mem. Am. Acad. Arts Sci.*, **10**, 9–351.
- Loysha, V.A., Krakovetsky, Yu.K. and Popov, L. N. (1989): Aurorae: Catalogue from IV to XVIII Centuries. *Acad. Sci. USSR Sov. Geophys. Comm.*, 1–125.
- Lyatsky, W., Newell, P.T. and Hamza, A. (2001): Solar illumination as cause of the equinoctial preference for geomagnetic activity. *Geophys. Res. Lett.*, **28**, 2353–2356.
- Matsusita, S. (1956): Ancient aurorae seen in Japan. *J. Geophys. Res.*, **61**, 297–302.
- Maunder, W. (1894): A prolonged sun-spot minimum. *Knowledge*, **17**, 173–176.
- Morooka, M. and Mukai, T. (2003): Density as a controlling factor for seasonal and altitudinal variations of the auroral particle acceleration region. *J. Geophys. Res.*, **108** (A7), 1306, doi: 10.1029/2002JA009786.
- Mozer, F.S., Cattell, C.A., Temerin, M., Torbert, R. B., Von Glinski, S., Woldorff, M. and Wygant, J. (1979): The DC and AC electric field, plasma density, plasma temperature, and field-aligned current experiments on the S3-3 satellite. *J. Geophys. Res.*, **84**, 5875–5884.
- Mukai, T., Kaya, N., Sagawa, E., Hirahara, M., Miyake, W., Obara, T., Miyaoka, H., Machida, S., Yamagishi, H., Ejiri, M., Matsumoto, H. and Itoh, T. (1990): Low energy charged particle observations in the “auroral” magnetosphere: First results from the Akebono (EXOS-D) satellite. *J. Geomagn. Geoelectr.*, **42**, 479–496.
- Murata, T., Matsumoto, H., Kojima, H. and Iyemori, T. (1997): Correlation of AKR index with  $Kp$  and  $Dst$  indices. *Proc. NIPR Symp. Upper Atmos. Phys.*, **10**, 64–68.
- Nakai, H. and Kamide, Y. (1999): Solar cycle variations in the storm-substorm relationship. *J. Geophys. Res.*, **104**, 22695–22700.
- Nevanlinna, H. and Pulkkinen, T.I. (1998): Solar cycle correlations of substorm and auroral occurrence frequency. *Geophys. Res. Lett.*, **25**, 3087–3090.
- Newell, P.T., Meng, C.-I. and Lyons, K.M. (1996): Suppression of discrete aurorae by sunlight. *Nature*, **381**, 766–767.
- Newell, P.T., Meng, C.-I. and Wing, S. (1998): Relation to solar activity of intense aurorae in sunlight and darkness. *Nature*, **393**, 342–344.
- Newell, P.T., Greenward, R.A. and Ruohoniemi, J.M. (1999): The role of the ionosphere in aurora and space weather. *Rev. Geophys.*, **39**, 137–149.
- Oya, H., Morioka, A., Kobayashi, K., Iizima, M., Ono, T., Miyaoka, H., Okada, T. and Obara, T. (1990): Plasma wave observation and sounder experiments (PWS) using the Akebono (EXOS-D) satellite-instrumentation and initial results including discovery of the high altitude equatorial plasma turbulence. *J. Geomagn. Geoelectr.*, **42**, 411–442.
- Persoon, A.M., Gurnett, D.A. and Shawhan, S.D. (1983): Polar cap densities from DE-1 plasma wave observations. *J. Geophys. Res.*, **88**, 10123–10136.
- Richardson, J.D., Paularena, K.I., Lazarus, A.J. and Belcher, J.W. (1995): Radial Evolution of the Solar Wind from IMP8 to Voyager 2. *Geophys. Res. Lett.*, **22**, 325–328.
- Richardson, J. and Wang, C. (1999): The global nature of solar cycle variations of the solar wind dynamic pressure. *Geophys. Res. Lett.*, **26**, 561–564.
- Schwabe, H. (1843): Solar observations during 1843. *Astron. Nachr.*, **21**, 233.
- Shelley, E.G., Sharp, R.D. and Johnson, R.G. (1976): Satellite observations of an ionospheric acceleration mechanism. *Geophys. Res. Lett.*, **3**, 654–656.
- Silverman, S.M. (1992): Secular variation of the auroral for the past 500 years. *Rev. Geophys.*, **30**, 333–351.
- Siscoe, G.L. (1980): Evidence in the aurora record for secular solar variability. *Rev. Geophys.*, **18**, 647–658.
- Spörer, F.W.G. (1889): Vierteljahrsschr. *Astron. Ges. Leipzig*, **22**, 323.
- Stothers, R. (1979): Ancient aurorae. *Isis*, **70**, 85–95.
- Tromholt, S. (1902): Katalog der in Nowegen bis Juni 1878 beobachteten Nordlichter. Kristiania, Oslo.

- Voots, G.R., Gurnett, D.A. and Akasofu, S.-I. (1977): Auroral kilometric radiation as an indicator of auroral magnetic disturbances. *J. Geophys. Res.*, **82**, 2259–2266.
- Wolf, R. (1856): Mitteilungen uber die Sonnenflecken. *Astron. Mitt. Zurich*, **1**, 8.
- Wolf, R. (1868): Mitteilungen uber die Sonnenflecken. *Astron. Mitt. Zurich*, **24**, 111.
- Wu, C.S. and Lee, L.C. (1979): A theory of the terrestrial kilometric radiation. *Astrophys. J.*, **230**, 621–626.
- Yamagishi, H., Fujita, Y., Sato, N., Stauning, P., Nishino, M. and Makita, K. (1998): Conjugate features of auroras observed by TV cameras and imaging riometers at auroral zone and polar cap conjugate-pair stations. *Polar Cap Boundary Phenomena*, ed. by J. Moen *et al.* Norwell, Kluwer Acad., 289–300.
- Yau, A.W., Walen, B.A., Peterson, W.K. and Shelley, E.G. (1984): Distribution of upflowing ionospheric ions in the high-altitude polar cap and auroral ionosphere. *J. Geophys. Res.*, **89**, 5507–5522.
- Yau, A.W., Beckwith, P.H., Peterson, W.K. and Shelley, E.G. (1985): Long-term (solar cycle) and seasonal variations of upflowing ionospheric ion events at DE 1 altitude. *J. Geophys. Res.*, **90**, 6395–6407.